X-ray Scattering Study on Amorphous, Polynuclear Platinum Uridine Complexes

Ritva Serimaa,[†,‡] Sakari Vahvaselkä,[†] Tarja Laitalainen,[*,§] Timo Paakkari,[†] and Anneli Oksanen[§]

Contribution from the Department of Physics, University of Helsinki, Siltavuorenpenger 20 D, 00170 Helsinki, Finland, and Department of Chemistry, University of Helsinki, Vuorikatu 20, 00100 Helsinki, Finland

Received February 18, 1993[⊗]

Abstract: The structures of amorphous, polynuclear platinum uridine complexes Pt–green **1** and **2**, Pt-violet **3**, Pt-blue **4**, and Pt-black **5** were studied by wide and small angle X-ray scattering methods (WAXS and SAXS) both as solids and in H_2O solution. The results of WAXS experiments showed differences in the degree of order between **1–5** in the solid state. The radical distribution functions (RDFs) for Pt complexes **1–5** from WAXS are in accord with a tetranuclear chainlike Pt structure in the solid state on the basis of the results of model calculations. The shortest average Pt–Pt distances varied from 3.00 to 3.08 Å for **1–5**, respectively. The Pt–N and Pt–O distances were 2.00–2.08 Å, and the corresponding coordination numbers were 4.5, 4.8, 4.5, 3.8, and 4.3 for **1–5**, respectively. The radii of gyration of **1–5** in H_2O solution (14 mg/mL) from SAXS analysis were 5, 4, 4, 9, and 7 Å, respectively. Pt-green **2** and Pt-violet **3** were found to exist rather as discrete dinuclear Pt units than as tetranuclear Pt units in H_2O solution. The double sizes of Pt-blue **4** and Pt-black **5** are interpreted as indicating the aggregates of the dinuclear Pt units.

1. Introduction

Tetranuclear crystalline platinum complexes have been synthesized from various model compounds related to pyrimidine nucleosides[1-7] in studies that tend to determine indirectly the structures of the group of antineoplastic, amorphous, polynuclear platinum coordination complexes known as platinum blues.[8,9] Structural information could be used in the development of the analogues of *cis*-Platin,[10] a well-established antitumor drug.

In spite of their antitumor activity, Pt-blues were withdrawn from clinical research due to the lack of repeatable syntheses. Later, evidence was given that the antitumor activity of Pt-blues might have arisen from the presence of decisively more active Pt-greens.[14] Today, there are selective syntheses only for "platinum pyrimidine blues"[11] and "platinum pyrimidine greens".[12,13] Even within the class of platinum pyrimidine greens, the nuclearity has been claimed to depend on reaction variables such as the temperature, and complexes containing eight to 28 Pt atoms have been obtained.[15,16] The size of the complex and its cytotoxic activity have been reported to vary as a function of the temperature.[17]

We have studied the structures of amorphous platinum uridine blues by means of wide and small angle X-ray scattering methods (WAXS, SAXS). WAXS and SAXS give direct structural information on both crystalline and amorphous materials. The atomic radial distribution function ($4\pi r^2\rho(r)$) can be determined from the WAXS data, which represents a distribution of neighboring atoms at distance r from an average atom in origin. The large scattering power of platinum allows identification of distances of Pt atoms from the radial distribution function (RDF). SAXS measurements gave information on particle sizes on the scale 5–500 Å. We used the SAXS results to estimate the average sizes of Pt units in H_2O solution.

We now report the results of WAXS and SAXS studies on amorphous platinum uridine complexes Pt-green **1** and **2**, Pt-violet **3**, Pt-blue **4**, and Pt-black **5**. Due to the tendency of the aging of the samples, the conditions after the syntheses were carefully controlled so that each sample had a known history. The results for Pt-green **1** and Pt-green **2** give an example of how sensitively the structure of the product depends on the details of the syntheses and storage. The experimental results are compared with the model calculations with 1-methyluracil blue.[27]

2. Experimental Section

2.1. Syntheses. Microanalyses were by Dornis und Kolbe, Mikroanalytisches Laboratorium, Germany. Visible spectra were taken by means of a Shimadzu UV-200 double-beam spectrometer and IR spectra by Nicolet 20xcs FTIR and Biorad FTS-7 FT-IR spectrometers. All the reagents were obtained from commercial sources and used without further purification. $[Pt(NH_3)_2(OH_2)_2]SO_4$ was prepared according to the

* To whom correspondence should be addressed.
† Department of Physics, University of Helsinki.
‡ Present address: Stanford Synchrotron Radiation Laboratory, Slac Bin 69, Stanford, P.O. Box 4349, CA 94305.
§ Department of Chemistry, University of Helsinki.
⊗ Abstract published in *Advance ACS Abstracts*, October 1, 1993.

(1) Barton, J. K.; Rabinowitz, D. J.; Szalda, D. J.; Lippard, S. J. *J. Am. Chem. Soc.* **1977**, *99*, 2827.
(2) Laurent, J.-P.; Lepage, P.; Dahan, F. *J. Am. Chem. Soc.* **1982**, *104*, 7335.
(3) Hollis, L. S.; Lippard, S. J. *Inorg. Chem.* **1983**, *22*, 2600.
(4) Matsumoto,K.; Fuwa, K. *J. Am. Chem. Soc.* **1982**, *104*, 897.
(5) Bernadelli, G.; Castan, P.; Soules, R. *Inorg. Chim. Acta* **1986**, *120*, 205.
(6) Sakai, K.; Matsumoto, K. *J. Am. Chem. Soc.* **1989**, *111*, 3074.
(7) Sakai, K.; Matsumoto, K.; Nishio, K. *Chem. Lett.* **1991**, 1081.
(8) Davidson, J. P.; Faber, P. J.; Fischer, R. G.; Mansy, S.; Peresie, H. J.; Rosenberg, B.; VanCamp, L. *Cancer Chemother. Rep., Part 1* **1975**, *59*, 287.
(9) Lippert, B. J. *Chem. Hematol. Oncol.* **1977**, *7*, 20.
(10) (a) Reedijk, J.; Fichtinger-Schepman, A. M. J.; van Oosterom, A. T.; van de Putte, P. *Structure and Bonding 67*; Springer-Verlag: Berlin, Heidelberg, 1987; pp 53–89. (b) Sunquist, W. I.; Lippard, S. J. *Coord. Chem. Rev.* **1990**, *100*, 293.
(11) Okuno, Y.; Tonosaki, K.; Inoue, T.; Yonemitsu, O.; Sasaki, T. *Chem. Lett.* **1986**, 1947.
(12) Shimura, T.; Tomohiro, T.; Laitalainen, T.; Moriyama, H.; Uemura, T.; Okuno, Y. *Chem. Pharm. Bull.* **1988**, *36*, 448.
(13) Laitalainen, T.; Okuno, Y.; Tomohiro, T. *Abstracts of the Fifth International Symposium on Platinum and Other Metal Coordination Compounds in Cancer Chemotherapy*, Abano Terme, Italy, 1987.
(14) Tomohiro, T.; Laitalainen, T.; Shimura, T.; Okuno, Y. *Proceedings of an International Symposium on Activation of Dioxygen and Homogeneous Catalytic Oxidations*, Tsukuba, Japan, July 12–16, 1987. *Stud. Org. Chem.* **1988**, *33*, 557–562.
(15) Okuno, Y.; Inoue, T.; Yonemitsu, O.; Tomohiro, T.; Laitalainen, T. *Chem. Pharm. Bull.* **1987**, *35*, 3074.
(16) Shimura, T.; Tomohiro, T.; Marumo, K.; Fujimoto, Y.; Okuno, Y. *Chem. Pharm. Bull.* **1987**, *35*, 5028.
(17) Okada, T.; Shimura, T.; Okuno, H. *Chem. Pharm. Bull.* 1992, *40*, 264.

0002-7863/93/1515-10036$04.00/0

literature from K_2PtCl_4[18] as a colorless 0.1 M solution, stored in a refrigerator, and used within 2 weeks. The ligand-to-Pt ratio was 1:1 in all the experiments. The reaction mixtures were gel filtered (Merck, Fractogel TSK HW-50(S)) by eluting with 0.012 M H_2SO_4. The preparations of platinum uridine blue[11] and greens[12] were carried out basically according to Okuno's procedure, with slight modifications. Since it was observed that very small changes may affect these materials, such as the wash with acetone, the preparations are described in detail.

Platinum Uridine Green 1. A mixture of $[Pt(NH_3)_2(H_2O)_2]SO_4$ (45 mL, 4.5 mmol), uridine (1.0989 g, 4.5 mmol), and hydrogen peroxide (82.8 μL, 30.5%) was heated in an oil bath at 70 °C under an argon atmosphere for 1 h and stirred at room temperature for an additional 1 h. The mixture was gel filtered, and the green zone was precipitated with acetone and kept in a refrigerator at 8 °C for 12 h. Filtering and drying under vacuum (0.01 mmHg) for 10 h gave 1.5386 g (69.8% of theory, based on Pt) of a green powder. Elemental anal. Found: C, 13.30; H, 3.25; N, 9.08; S, 6.19; Pt, 39.85. Visible (H_2O): λ_{max} 730 nm. IR (KBr): 1625 cm^{-1} (C=O).

Platinum Uridine Green 2. A mixture of $[Pt(NH_3)_2(H_2O)_2]SO_4$ (40 mL, 4.0 mmol), uridine (0.9768 g, 4.0 mmol), and hydrogen peroxide (73.6 μL, 31.3%) was heated in an oil bath at 52–54 °C for 2 h under argon and stirred at room temperature for an additional 2 h. The green zone was dropped directly into a 10-fold amount of acetone and allowed to precipitate at 8 °C for 12 h. Acetone was poured off and fresh acetone added to ease the detachment of the product adhered to the bottom of the conical flask. Through this procedure, the tarry produce became loose and easy to handle. The material was washed with acetone and dried under vacuum (0.01 mmHg) for 12 h to give 1.4267 g (77.9% of theory, based on Pt) of a green powder. Elemental anal. Found: C, 15.02; H, 3.43; N, 9.22; S, 4.68; Pt, 42.63. Visible (H_2O): λ_{max} 730 nm. IR (KBr): 1625 cm^{-1}.

Platinum Uridine Violet 3. A mixture of $[Pt(NH_3)_2(H_2O)_2]SO_4$ (30 mL, 3.0 mmol) and uridine (0.7326 g, 3.0 mmol) was stirred at room temperature under an argon atmosphere for 170 h. The only colored zone, violet, was precipitated with acetone. After 12 h at 8 °C the product was washed with acetone (200 mL), which made the filtrate slightly turbid. Drying under vacuum (0.01 mmHg) for 10 h gave 1.0511 g of a bluish gray powder (67.6% of theory, based on Pt). Elemental anal. Found: C, 18.26; H, 3.35; N, 9.80; S, 4.10; Pt, 37.64. Visible (H_2O): λ_{max} 717, 555, 482 nm. IR (KBr): 1635 cm^{-1} (C=O).

Platinum Uridine Blue 4. Pt-blue was prepared basically according to Okuno's procedure,[11] with the difference that we used $PtI_2(NH_3)_2$ instead of $PtCl_2(NH_3)_2$ and we used acidic conditions without light protection. A mixture of $[Pt(NH_3)_2(H_2O)_2]SO_4$ (10 mL, 1.0 mmol) and uridine (0.2442 g, 1.0 mmol) was heated at 70–73 °C under air for 16 h and stirred at room temperature for an additional 7 h in a stoppered transparent flask. The blue zone was precipitated with a 10-fold amount of acetone and kept at 8 °C for 12 h. The product did not adhere to the bottom of the conical flask like Pt-green and Pt-violet. Washing with acetone and drying under vacuum (0.01 mmHg) for 10 h gave 0.375 g of a blue powder (67.7% of theory, based on Pt). Elemental anal. Found: C, 18.90; H, 3.53; N, 9.20; S, 3.88; Pt, 35.22. Visible (H_2O): λ_{max} 567 nm (broad, unsymmetrical). IR (KBr): 1635 cm^{-1} (C=O).

Platinum Uridine Black 5. Platinum uridine green **1** was dissolved in deionized water (4:1 w/w), and the water was allowed to evaporate during 24 h from an open vessel at room temperature to give a brittle and tarry product, Pt-black **5**. The weight gain in the transformation from Pt-green to Pt-black was 4%, which means roughly 1 H_2O: 1 Pt atom. Elemental anal. Found: C, 14.44; H, 4.11; N, 9.08; S, 5.05; Pt, 34.21. Visible (H_2O): λ_{max} 723 (broad) and 494 nm. IR (KBr): 1622 cm^{-1} (C=O).

2.2. Sample Preparation and Stability in X-ray Scattering Measurements. In order to confirm the repeatability of the study, we measured the Pt complexes **1–5** twice and the samples were from separate reactions. We did not observe any significant changes in the RDFs. We measured Pt-green **1** 3 days after the synthesis and storage in a transparent desiccator over $CaCl_2$, and Pt-green **2** 1 day, Pt-violet **3** 3–4 days, Pt-blue **4** 2–3 days, and Pt-black **5** 1 day after the syntheses and storage at room conditions. We found out that dry Pt-green **1** is hygroscopic[19,20] and observed small changes in the RDF after 2 days exposure to room conditions.[19] The RDF of a 6-month-old sample of Pt-green **2** is essentially the same as the result presented in this work. The same samples or the same products of the Pt complexes were used for both SAXS and WAXS measurements. The samples were made by pressing the finely divided dry amorphous material into pellets of the size 10 × 40 × 3 mm^3. To avoid a deterioration of the sample due to moisture and to diminish the portion of nonsample scattering, the WAXS experiments were carried out in a vacuum (0.004 mbar). The solutions were prepared in deionized H_2O 0.5–1.0 h before the SAXS measurements. The color of the sample was visually checked after each measurement. The stability of the sample was verified by using consecutive scans (1800–3600 s), and no significant changes in the intensity curves were observed.

Table I. The Shortest Pt–Pt Distances (Å) in 1-Methyluracil Blue[27] Compared to Experimental Interatomic Distances of Pt-violet **3**[a]

numbering scheme for tetranuclear Pt complexes	1-methyluracil blue[27]	Pt-violet **3**
Pt1–Pt2, Pt3–Pt4	2.79, 2.81	2.98
Pt2–Pt3	2.87	2.98
Pt2–Pt4, Pt1–Pt3	5.61, 5.63	4.9, 5.5
Pt1–Pt4	8.5	8.2
Pt4–Pt1′	4.9	4.3
Pt3–Pt1′, Pt4–Pt2′	7.51, 7.57	7.4

[a] The Pt atoms are labeled as shown in Figure 6. The primes refer to the neighboring tetranuclear Pt unit.

2.3. Wide-Angle X-ray Scattering. 2.3.1. Measurements and Data Evaluation. The wide angle X-ray scattering experiments were carried out by using the symmetrical reflection geometry with Mo $K\alpha_1$ radiation from a sealed fine focus X-ray tube (2 kW) connected to a Siemens power unit (Kristalloflex 710H). Almost pure Mo $K\alpha_1$ radiation containing only 7% of the Mo $K\alpha_2$ component was obtained by using reflection 220 of a singly bent silicon monochromator crystal.[21] The scattered radiation was detected by a HPGe solid-state detector.

The experimental (WAXS) intensity curves were corrected for polarization and absorption. The intensity curves were normalized to absolute scale, and the portion of Compton scattering was removed. The normalization could be made successfully with both the large-angle and the integral method.[22,23] The scattering factors and dispersion correction terms were taken from *International Tables for X-ray Crystallography*[24] and incoherent scattering functions from a manuscript of its new edition.[25]

2.3.2. Interpretation of Results Based on Model Calculations. The X-ray scattering from amorphous materials can be expressed in terms of the partial distribution functions ρ_{ab} (PDFs), which represent the average atomic density of b atoms a distance r away from an a atom. From a measured intensity curve the total radial distribution function $4\pi r^2\rho(r)$ (RDF), which is a weighted sum of the PDFs, can be determined. The RDF is related to X-ray scattering as follows:[26]

$$4\pi r^2\rho(r) = 4\pi r^2\rho_0 + (2/\pi)\, r \int_0^\infty ki(k) \sin kr \, dk$$

where ρ_0 is the average atomic density and $i(k)$ is the total structure function, which is calculated from the coherently scattered intensity per atom I_a by

$$i(k) = \frac{I_a - \langle f^2 \rangle}{\langle f \rangle^2}$$

where $\langle f^2 \rangle$ is the coherent independent intensity and $\langle f \rangle$ the average scattering factor for the unit of composition.

The experimental results are interpreted on the basis of model calculations. The crystal structure of tetranuclear 1-methyluracil blue[27] was chosen due to its close structural similarity to uridine. Its unit cell is triclinic, with lattice constants a = 10.123 Å, b = 13.084 Å, c = 19.508 Å, α = 92.280°, β = 101.090°, and γ = 107.490°. The shortest Pt–Pt distances of the model compound are presented in Table I. The shortest Pt–N and Pt–O distances of 1-methyluracil blue[27] are 2.04–2.08 Å.

(18) Dhara, S. C. *Indian J. Chem.* **1970**, *8*, 193.
(19) Serimaa, R.; Vahvaselkä, S.; Paakkari, T.; Laitalainen, T.; Sundberg, M.; Oksanen, A. University of Helsinki, Report Series in Physics, HU-P-254; 1990.
(20) Goodgame, D. M. L.; Jeeves, J. *Z. Naturforsch.* **1979**, *34C*, 1287.
(21) Vahvaselkä, S.; Mangs, J. *Physica Scripta* **1988**, *38*, 737.
(22) Norman, N. *Acta Crystallogr.* **1957**, *10*, 370.
(23) Krogh-Moe, J. *Acta Crystallogr.* **1956**, *9*, 951.
(24) *International Tables for X-ray Crystallography*; The Kynoch Press: Birmingham, England, 1974.
(25) Alexandropolous, N. G.; Cooper, M. J. Contribution (1986) to the new edition of *International Tables for X-ray Crystallography*, to be published.
(26) Zernike, F.; Prins, J. A. *Z. Phys.* **1927**, *41*, 184.
(27) O'Halloran, T. V.; Mascharak, P. K.; Williams, I. D.; Roberts, M. M.; Lippard, S. J. *Inorg. Chem.* **1987**, *26*, 1261.

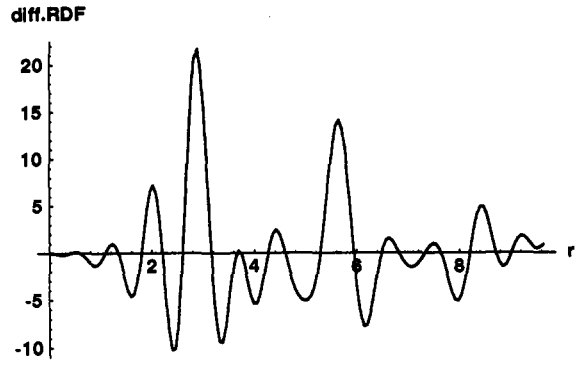

Figure 1. The calculated ΔRDF of one tetranuclear Pt unit of $[(NH_3)_2Pt(1\text{-methyluracil})Pt(NH_3)_2]_2(NO_3)_5$ from simulated WAXS data.

Figure 1 shows the difference radial distribution function, $\Delta RDF = 4\pi r^2[\rho(r) - \rho_0]$, of a tetranuclear Pt unit of 1-methyluracil blue.[27] The intensity curve of this Pt unit was first calculated by using the classical Debye formula[28] excluding thermal vibrations, and the ΔRDF was calculated from the intensity curve in the same way as the experimental ones by using the same step width and the same range of k. The nitrate counterions were included, but their effect on the intensity curve is negligible. According to Figure 1, the most significant features of the ΔRDF are the maxima arising from the Pt–Pt distances. If a sample consists of randomly distributed tetranuclear Pt units, the three maxima of the ΔRDF corresponding to the Pt–Pt distances are easily identifiable.

The maxima of the model RDF at about 2 and 3 Å are partially due to the shortest Pt–N, Pt–O, and Pt–Pt distances and partially due to distances between N, O, and C atoms. For interpretation of the average coordination numbers (CNs), we approximate the Pt complexes as a two-component system of Pt and the elements C, N, O, and S. The shares of the PDFs in the total RDF of a two-component system are approximately[29]

$$\mathrm{RDF} \approx \frac{x_a f_a^2 \rho_{aa} + 2x_a f_a f_b \rho_{ab} + x_b f_b^2 \rho_{bb}}{(x_a f_a + x_b f_b)^2}$$

where x_a and x_b are atom fractions of components a and b. The shares are roughly ($x_{Pt} \approx 0.03$, $f_{Pt} \approx |f_{Pt}(0)| \approx 76$, and $f_{C,N,O,S} \approx 4.5$)

$$\mathrm{RDF} \approx 3.1\rho_{Pt\text{–}Pt} + 0.4\rho_{Pt\text{–}others} + 0.5\rho_{others\text{–}others}$$

At 2 Å the CN due to distances of Pt atoms and other elements (N, O, C, S, H) in the sample is probably more than 80%, because the contribution of the distances of pairs of C, N, and O atoms remains probably less than 20%. The shortest Pt–C distances are not discernible separately in the RDFs, and these distances likely contribute to the CN at 3 Å. In a di- or tetranuclear Pt complex there are likely four to six C, N, and O atoms at a distance of 3 Å from the Pt atom, and the CN due to distances between pairs of C, N, and O atoms may be about 4. The CN at 3 Å is about 8, 10, and 12 for dinuclear, tetranuclear, and polynuclear chainlike Pt complexes, respectively. Because the contribution of Pt–Pt distances to the CN at 3 Å may be only 50%, the exact nuclearity of the Pt complexes cannot be determined unambiguously merely on the basis of the CNs.

2.3.3. Experimental Results. Figure 2 shows the experimental coherent intensities of **1**, **2**, and **5**, and Figure 3 shows the total structure functions of **1**–**5**. The intensity curves of **1**–**5** differ to a certain degree from each other at small values of k. The intensity curves of Pt-blue **4** and Pt-black **5** display the sharpest features and consequently the highest degree of order, while Pt-green **2** shows the lowest degree of order.

The ΔRDFs in Figure 4 all display noticeable maxima at about 2, 3, and 4–6 Å, which indicate a structural similarity of the Pt units with the model (Figure 1). The statistical precision of the intensity curves was better than 1%, which means that the ΔRDFs are reasonably accurate up to about 9 Å.[19] The interatomic distances, which were determined as positions of the maxima of the ΔRDFs, are presented in Table II. The CNs, which were determined as the areas of the maxima of the RDF, are given in Table III. The maxima of the RDFs are not resolved well enough that the precision of the determination was better than 10%.

The comparison of the RDFs of Pt-green **1** and **2** reveals differences in the position of the maxima and in the CNs. The maximum of the RDF of **1** at 3 Å is broader than that in **2**, and the maxima between 3.5–4.5 Å deviate slightly from each other, too. The nuclearity of **1** is likely not higher than that of **2** even though it has a larger CN at 3 Å. Since the maximum at 3 Å of the RDF of **1** is broad, it may contain two Pt–Pt distances or the contribution of elements other than Pt may be larger. The shift of the maximum at 5.2 Å in the RDF of **1** to 5.4 Å in that of **2** is also noticeable.

The CNs at 2 Å of Pt-green **2** and Pt-blue **4** differ from those of the Pt complexes **1**, **3**, and **5** (4.3–4.5), which may indicate that the amounts of the H_2O and the NH_3 ligands vary in the Pt complexes **1**–**5**. The CN at 3 Å of Pt-green **2** (9) is smaller than the CNs of the other Pt complexes (10.8–11.9). The average Pt–Pt distance was 3.05 Å for Pt-green **2** and Pt-blue **4** and slightly shorter for the Pt complexes **2**, **3**, and **5**. All the ΔRDFs have a less intensive maximum at 4.2–4.3 Å. The ΔRDFs of the Pt complexes **2** and **3** have one intensive maximum, and the ΔRDFs of the Pt complexes **1**, **4**, and **5** have two of them in the range 4.9–6.0 Å. Pt-green **2** and Pt-blue **4** have a maximum at 7.7–7.8 Å, and Pt-green **1**, Pt-violet **3**, and Pt-black **5** at 8.2–8.3 Å.

2.4. Small-Angle X-ray Scattering. 2.4.1. Measurements and Data Evaluation. The small angle X-ray scattering experiments were carried out with Cu Kα radiation monochromatized by means of a total reflecting mirror (Huber small-angle chamber 701) and Ni filter. Radiation for SAXS measurements was obtained from a sealed Cu anode fine focus

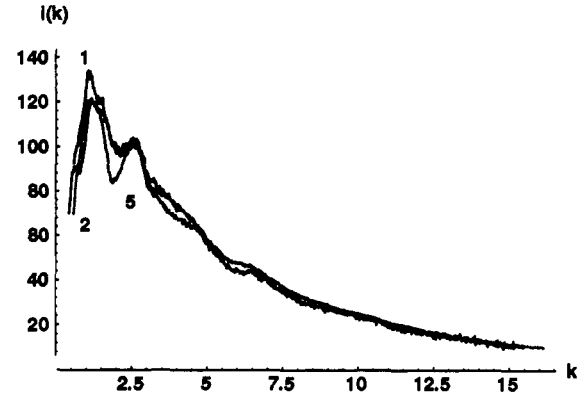

Figure 2. The experimental coherent intensities (WAXS) of Pt-green **1**, Pt-green **2** (gray), and Pt-black **5**.

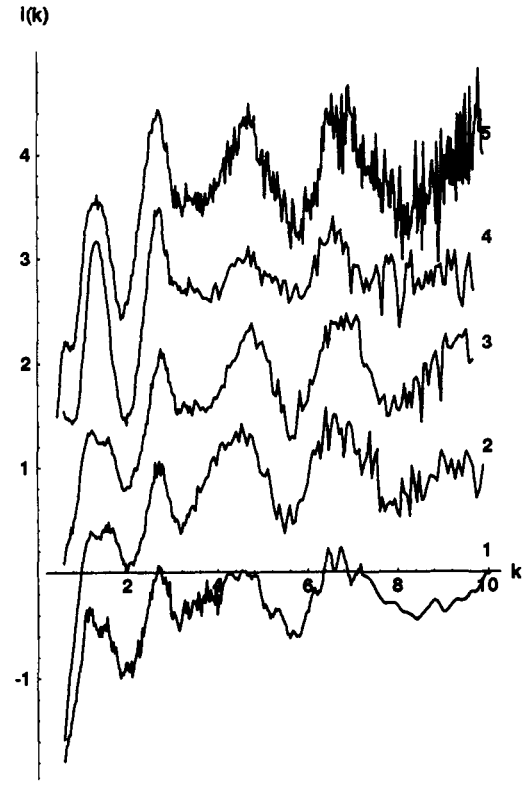

Figure 3. The total structure functions of Pt-green **1**, Pt-green **2**, Pt-violet **3**, Pt-blue **4**, and Pt-black **5** from WAXS data.

(28) Debye, P. *Ann. Phys. (Leipzig)* **1915**, *46*, 809.
(29) Ding, K.; Andersen, H. C. *Phys. Rev.* **1987**, *B36*, 2675.

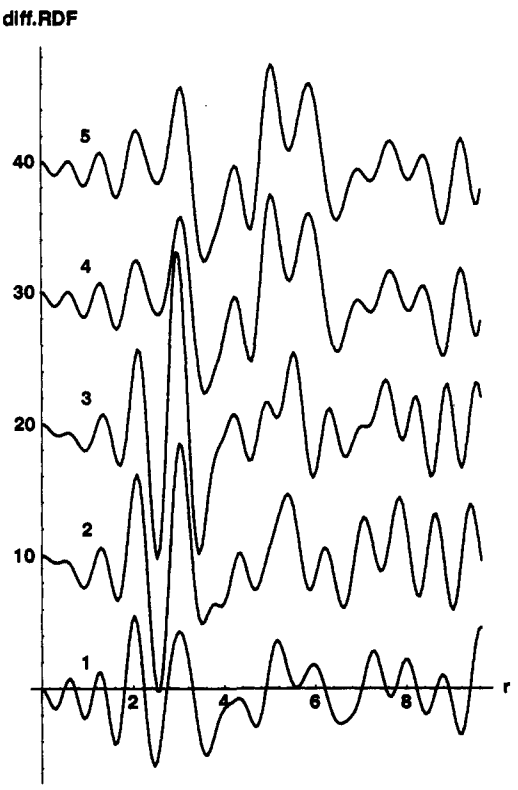

Figure 4. The experimental ΔRDFs of Pt-green **1**, Pt-green **2**, Pt-violet **3**, Pt-blue **4**, and Pt-black **5** from WAXS data.

Table II. Experimental Interatomic Distances (Å) in the Range 2.0–8.5 Å Determined from the Most Pronounced Maxima of the ΔRDFs

Pt-green **1**	2.03	3.00	4.3	5.2	5.9	7.3	8.0
Pt-green **2**	2.05	3.05	4.3		5.4	7.8	
Pt-violet **3**	2.10	2.98	4.2	4.9	5.5	7.5	8.2
Pt-blue **4**	2.08	3.05	4.3	5.1	5.9	7.7	
Pt-black **5**	2.03	2.95	4.2	5.0	6.0	7.4	8.3

Table III. Experimental Average Coordination Numbers (CNs) at 2 and 3 Å[a]

	CN	
Pt complex	2 Å	3 Å
Pt-green **1**	4.5	11.9
Pt-green **2**	4.8	9.0
Pt-violet **3**	4.5	11.5
Pt-blue **4**	3.8	11.2
Pt-black **5**	4.3	10.8

[a] The CNs are calculated as the areas of the maxima of the RDFs. The average atomic density was 0.1 $Å^{-3}$.

X-ray tube powered by a Siemens Kristalloflex 710H unit. The scattered radiation was detected by a linear one-dimensional position-sensitive proportional counter (MBraun OED-50M). A narrow slit (1 mm) was installed in front of the detector window.

The sample container was a narrow (0.8 mm) cavity in a steel frame with thin stretched polypropylene foils as flat faces (6 μm).[30] The intensities of the solvent and the foils were measured separately. The duration of the measurement was 0.5–1.0 h, and the reliable range of k was 0.03 $Å^{-1} \leq k \leq 0.6$ $Å^{-1}$.

To extract the intensity of small-angle scattering of the Pt complexes **1**–**5**, the contributions of the solvent and the foils were eliminated.[31] The primary beam is narrow (FWHM ≤ 0.008 $Å^{-1}$) compared to its height, and the instrumental smearing effect due to the beam width is negligible in comparison to that of the beam height (FWHM ≈ 0.16 $Å^{-1}$). The

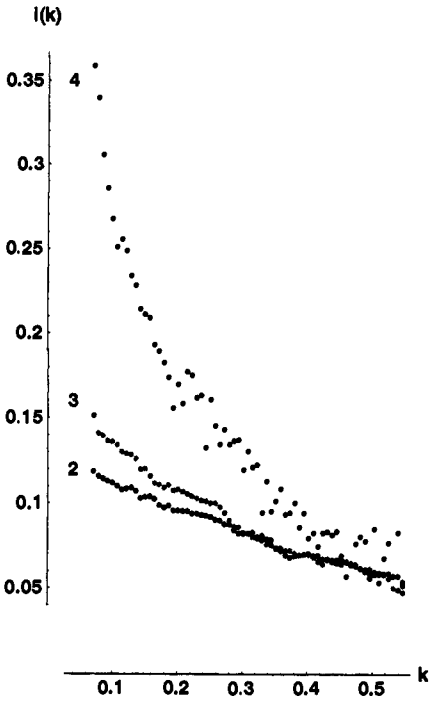

Figure 5. The experimental SAXS intensity curves (arbitrary units) of Pt-green **2**, Pt-violet **3**, and Pt-blue **4**.

smearing effect caused by the beam height was removed by using an iterative procedure of Lake.[32] The intensity curves were broad, indicating that the scattering units are small. The intensity curves behaved according to the Guinier approximation in the interval 0.03 ≤ k ≤ 0.15 $Å^{-1}$.

2.4.2. Results. For materials consisting of isolated particles in solution, the average radius of gyration of particles,

$$R_g^2 = {}^1/_2\left(\int \gamma(r) r^6 \, dr\right)/\left(\int \gamma(r) r^2 \, dr\right)$$

where $\gamma(r)$ is the autocorrelation function of the electron density of the particle, is obtained from the innermost part of the intensity curve by means of the Guinier approximation[33] as

$$I(k) = I(0) \exp(-k^2 R_g^2/3)$$

For the interpretation of the results, the dependence of the sizes of the particles as a function of concentration was studied. The intensity curves of Pt-green **1**, Pt-violet **3**, Pt-blue **4**, and Pt-black **5** depended only weakly on concentration between 14 and 140 mg/mL, 7 and 140 mg/mL, and 14 and 140 mg/mL respectively. The intensity curves of Pt-green **2** and Pt-blue **4**[34] displayed a clear variation in the intensity curves between 14 and 140 mg/mL and 1.4 and 9.8 mg/mL, respectively. The dependence of the shape of the intensity curve on concentration arises rather from aggregation of the particles than from interparticular interference effects in a solution of discrete particles of equal size.

Figure 5 presents the intensity curves of Pt-green **2**, Pt-violet **3**, and Pt-blue **4**, and the experimental radii of gyration R_g for the concentration 14 mg/mL are given in Table IV. The R_g's of one dinuclear, one tetranuclear, and two associated tetranuclear Pt units of 1-methyluracil blue[27] are compared with the experimental values in Table IV. The value of R_g depends on the shape of the Pt unit. The R_g's of aggregates of four dinuclear Pt units may vary between 8 and 11 Å, depending on the shape of the aggregate. The R_g's of Pt-green **2** and Pt-violet **3** are about the same as that of a single dinuclear Pt unit, and the R_g of Pt-green **1** is about the same as that of a tetranuclear Pt unit. The R_g's of Pt-blue **4** and Pt-black **5** are in the range of R_g's of aggregates of two tetranuclear Pt units. On the basis of our computer simulations[34] for Pt-blue **4**, we propose that small-angle scattering arises from aggregates of two to five dinuclear Pt units for both Pt-blue **4** and Pt-black **5**.

(30) Vahvaselkä, S. University of Helsinki, Report Series in Physics, HU-P-257, 1992.
(31) Müller, K. In *Small Angle X-ray Scattering*; Glatter, O., Kratky, O., Eds.; Academic Press Inc.: London, 1982; 229–232.
(32) Lake, J. *Acta Crystallogr.* **1967**, *23*, 191.
(33) Guinier, A.; Fournet, G. *Small-Angle Scattering of X-rays*; John Wiley & Sons, Inc.: New York, 1955.
(34) Serimaa, R.; Laitalainen, T.; Vahveselkä, S.; Paakkari, T. *Inorg. Chim. Acta*, submitted for publication.

Table IV. Experimental Radii of Gyration (R_g's) with the Calculated Values for 1-Methyluracil Blue[27] [a]

Experimental R_g (Å)	
Pt-green **1**	5
Pt-green **2**	4
Pt-violet **3**	4
Pt-blue **4**	9
Pt-black **5**	7
Calculated R_g (Å)	
1 dinuclear Pt unit	4
1 tetranuclear Pt unit	5
aggregates of 2 tetranuclear Pt units	8

[a] The calculated R_g's were determined from the intensity curves of randomly distributed dinuclear Pt units, tetranuclear Pt units, and an aggregate of two tetranuclear Pt units of the model compound.

3. Discussion

The wide angle X-ray scattering method has rarely been used for the structural studies of Pt-blues[36] and never for Pt-nucleobase blues. In an EXAFS study of Pt-uridine blue,[35] the Pt–Pt distance of about 3 Å has been determined earlier. Our WAXS data shows that the complexes **1–5** are amorphous, but the degree of order varies slightly. According to earlier studies, Pt-blues represent mixtures of various amorphous monomeric and polymeric species.[37–42] X-ray scattering methods give averaged structural data on the whole irradiated sample. On the basis of the number and the width of the maxima in the RDFs, Pt complexes **2–5** represent a case with one dominant Pt structure and Pt-green **1** may be a kind of mixture, though the differences in the data are small.

Because the difference between scattering factors of N and O is very small and the shortest Pt–N and Pt–O distances are nearly equal, it is not possible to differentiate between the N and O ligands on the basis of the coordination number at 2 Å. Several reactions such as hydrolysis of ammonia,[43–47] interconversion between head–head and head–tail configurations of the dinuclear Pt units, and any substitutions in the coordination sphere of Pt, where only the coordinating element between N and O is varied, can take place without noticeable change in the coordination number at 2 Å.

The dominating features of the experimental RDFs of the Pt complexes **1–5** are the intensive maxima at 3 and 5–6 Å. These maxima are intensive enough to arise from Pt–Pt distances, which indicates that the Pt structure of the Pt complexes **1–5** is at least dinuclear. A slight variation in the position of this maximum (Figure 4) does not necessarily indicate that the shortest Pt–Pt distance varies. The variation may also arise from differences in the average Pt–N, Pt–O, and Pt–C distances contributing to the maximum at 3 Å.

For further interpretation of the results, the ΔRDFs (Figure 4) are discussed on the basis of the four models (Figures 6 and 7). Figure 6 shows the detailed structure of the crystalline

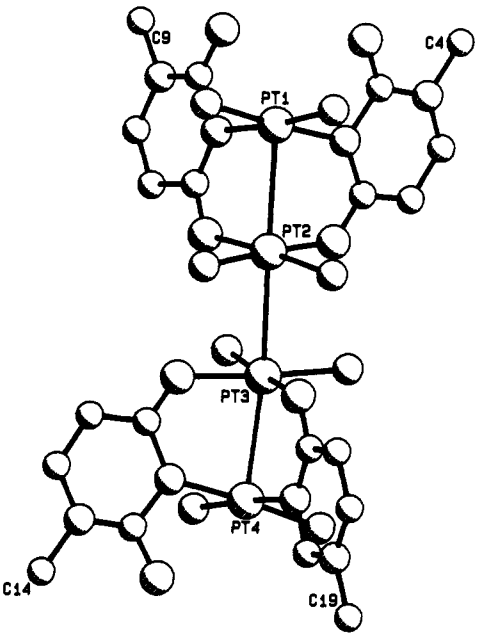

Figure 6. One tetranuclear Pt unit of $[(NH_3)_2Pt(1\text{-methyluracil})Pt(NH_3)_2]_2(NO_3)_5$. Hydrogen atoms are omitted for clarity.

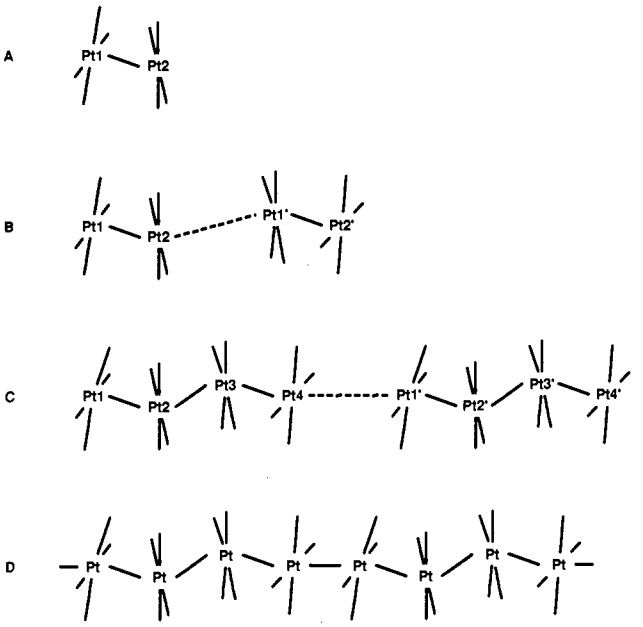

Figure 7. Models for Pt structures of amorphous Pt-uridine complexes: (A) a dinuclear Pt unit, (B) associated dinuclear Pt units, (C) associated tetranuclear Pt units, and (D) a polynuclear Pt unit. Pt–Pt distances of about 3 Å are denoted by a solid line and longer Pt–Pt distances by a dashed line.

tetranuclear model molecule[27] used for calculations, although the hydrogen atoms are omitted for clarity. Figure 7 presents the Pt structures of the following models A–D. Model A consists of randomly distributed discrete dinuclear Pt units. Model B consists of associated dinuclear Pt units, with the closest interdimeric distance of 4.9–6 Å (Pt2–Pt1′) between the Pt atoms. Model C consists of tetranuclear Pt units, with the shortest distance of two tetranuclear units (Pt4–Pt1′) larger than 3 Å. Model D consist of polynuclear chainlike Pt units, with the distance of all neighboring Pt atoms of about 3 Å. The atoms are numbered according to Figure 7. Numbers with primes indicate atoms in an adjoining Pt unit in respective order.

Model A is ruled out because the experimental ΔRDFs should contain only one intensive maximum at about 3 Å, which is not the case. Model B, consisting of adjoining dinuclear Pt units

(35) Teo, B.-K.; Kijima, K.; Bau, R. *J. Am. Chem. Soc.* **1978**, *100* (2), 621.
(36) Korsumski, V. I.; Muraveiskaja, G. S.; Abashkin, V. E. *Russ. J. Inorg. Chem. (Engl. Transl.)* **1988**, *33*, 669.
(37) Zaplatynski, P.; Neubacher, H.; Lohmann, W. *Z. Naturforsch.* **1979**, *34b*, 1466.
(38) Farrell, N. *Transition metal complexes as drugs and chemotherapeutic agents*. Kluwer Academic Publishers: The Netherlands, 1989.
(39) Woollins, J. D.; Rosenberg, B. *Inorg. Chem.* **1982**, *21*, 1280.
(40) Laurent, M. P.; Tewksbury, J. C.; Krogh-Jespersen, M.-B.; Patterson, H. *Inorg. Chem.* **1980**, *19*, 1656.
(41) Burness, J. *Inorg. Chim. Acta* **1980**, *44*, L49.
(42) Flynn, C. M.; Wiswahathan, T. S.; Martin, R. B. *J. Inorg. Nucl. Chem.* **1977**, *39*, 437.
(43) Norman, R. E.; Ranford, J. D.; Sadler, P. J. *Inorg. Chem.* **1992**, *31*, 877.
(44) Lipiński, J. *J. Mol. Struct.* **1989**, *201*, 295.
(45) Lippert, B.; Schöllhorn, H.; Thewalt, U. *Inorg. Chem.* **1986**, *25*, 407.
(46) Bauer, W.; Gonias, S. L.; Kam, S. K.; Wu, K. C.; Lippard, S. J. *Biochemistry* **1978**, *17*, 1061.
(47) Hiltunen, Y.; Laitalainen, T.; Serimaa, R.; Oksanen, A.; Rahkamaa, E. To be published.

with interdimer Pt–Pt distances around 4.9–6 Å (Pt2–Pt1′) and 7.5–8.5 Å (Pt1–Pt1′, Pt2–Pt2′), would also explain the second and the third maximum in the ΔRDFs. However, the experimental CNs at 3 Å (9–11.9) are considerably larger than the calculated value for models A and B, 8, which rules out also model B.

The tetranuclear model C agrees well with the positions of the maxima of the ΔRDFs. The maxima at 3, 4.9–6, and 7.5–8.5 Å can arise from one tetranuclear Pt unit alone, assuming spacings of about 3 Å between adjoining Pt atoms (Pt1–Pt2, Pt2–Pt3, and Pt3–Pt4), a spacing of 4.9–6 Å between Pt1–Pt3 and Pt2–Pt4, and a spacing of 7.5–8.5 Å for Pt1–Pt4. Also, the intensities of these maxima are quite well explained with a model of one tetranuclear unit. The calculated average CN for this model is about 10 at 3 Å, which compares well with the experimental results of 9–11.9, given in Table III. The calculated contributions of Pt–Pt distances to the CNs at 4.9–6 and 7.5–8.5 Å are 0.5 and 0.25. This is also in agreement with the experimental results for the intensities of the maxima (Figure 1).

Furthermore, the less intensive maximum between 4.9 and 6 Å in ΔRDFs of the complexes **1**, **4**, and **5** or the maximum at 4.2–4.3 Å in all ΔRDFs may refer to the shortest Pt–Pt distance between two tetranuclear units (Pt4–Pt1′). As an example, the experimental ΔRDF of Pt-violet **3** was interpreted according to this model (Table I). This would mean that even though the materials are amorphous, there might be some order between the tetranuclear Pt units.

Model D, a polynuclear chainlike structure, where the distance of neighboring Pt atoms is about 3 Å, can also explain the positions of the intensive maxima of the experimental ΔRDFs, but fails to interpret the intensities. According to the model calculations, the average CN at 3 Å of a polynuclear chain (D) should be about 12, which is larger than the experimental values (Table III). The maxima of the experimental ΔRDFs at 7.5–8.5 Å should also be more intensive to fit with model D,[19] since the Pt–Pt CNs at 3, 4.9–6, and 7.5–8.5 Å should all be close to 2 in a long Pt chain.

Aqueous solutions of Pt-blues have not been studied earlier by means of small-angle X-ray scattering (SAXS). The solution chemistry of di- and tetranuclear Pt complexes under redox conditions has been advanced by Lippard et al.[48,49] and Matsumoto et al.[50] The studies[48] indicate that tetranuclear Pt units may decompose in solution. According to the SAXS data, Pt-green **2** and Pt-violet **3** show this tendency most clearly (Table IV). That Pt complexes **1**–**3** exist mainly either as dinuclear or tetranuclear Pt units in the concentration of 14 mg/mL is in contradiction with Pt molecules reported for platinum uridine greens, which have eight to 28 Pt atoms is a polynuclear complex.[16] Only in the case of Pt-blue **4** and Pt-black **5** is a larger size than that of one tetranuclear unit justified and even then only up to two adjoining tetranuclear units.

Structural data is needed to control the chemistry of platinum blues, which is still a challenge. Both the observed structural similarity of the variously colored Pt-uridine complexes in the solid state and the differences in the sizes of the aggregates and in the tendency of aggregation in H_2O solutions are interesting results which deserve further study. It is possible that the principal factor of biological activity of Pt-greens arises from aggregation and the phenomenology of mixed-valent Pt complexes is due to aggregation, as well.

4. Concluding Remarks

The di- and tetranuclear basic structures were determined for the first time for amorphous platinum uridine complexes **1**–**5** in the family of "platinum blues" from the atomic radial distribution functions by WAXS and the approximate sizes of **1**–**5** by SAXS. The complexes **1**–**5** exist in the solid state as tetranuclear and in H_2O solution as di- or tetranuclear Pt units or as aggregates of dinuclear Pt units. The structural similarity of platinum blues with the crystalline model compounds has now been confirmed, and it is in accord with the conclusions reached by other researchers about the chemical similarity between crystalline and amorphous platinum blues with a multitude of methods.

Acknowledgment. The financial support of the Academy of Finland, the Neste Foundation, the Technology Development Centre, and the University of Helsinki is gratefully acknowledged.

Supplementary Material Available: Total structure functions, ΔRDFs, and experimental coherent intensities as a function of k (1/Å) (15 pages). Ordering information is given on any current masthead page.

(48) Barton, J. K.; Caravana, C.; Lippard, S. J. *J. Am. Chem. Soc.* **1979**, *101*, 7269.
(49) Hollis, L. S.; Lippard, S. J. *J. Am. Chem. Soc.* **1983**, *105*, 3494.
(50) Abe, T.; Moriyama, H.; Matsumoto, K. *Inorg. Chem.* **1991**, *30*, 4198.